The lithospheric to lower mantle carbon cycle recorded in superdeep diamonds

M.E. Regier[1]*, D.G. Pearson[1], T. Stachel[1], R.W. Luth[1], R. A. Stern[1], J.W. Harris[2]

[1]Canadian Centre for Isotopic Microanalysis, Department of Earth and Atmospheric Sciences, University of Alberta, Edmonton AB, Canada. [2]University of Glasgow, School of Geographical and Earth Sciences, Glasgow, G12 8QQ, UK

The transport of carbon into Earth's mantle is a critical variable in the global carbon cycle, which affects both climate fluctuations and the redox conditions of the surface and mantle. The largest unconstrained variables in this cycle are the depth to which carbon in subducting sediments and altered oceanic crust remains stable, and the relative roles of these components in removing carbon from the cycle by sequestering it in the deep mantle [1]. Inclusions in sublithospheric, or superdeep diamonds (derived from >250 km) provide an unparalleled avenue from which to study these questions. Here we present oxygen isotopic measurements of mineral inclusions within diamonds from Kankan, Guinea. These inclusions are derived from a ~ 700 km deep cross section of the mantle from lithosphere to uppermost lower mantle. Along with a large isotopic database of diamond hosts, these data track a predominately altered oceanic crust reservoir for carbon in slabs at lithospheric to transition zone depths. While the oxygen isotopic compositions of inclusions in eclogitic diamonds from the cratonic lithosphere are representative of the altered oceanic crust that now exists as eclogite pods within the cratonic mantle root, inclusions in sublithospheric diamonds from ~300 to ~600 km depths, have more extreme isotopic signatures. These extreme values indicate that carbonate-rich subducting slabs undergo melting at these depths. In contrast, lower mantle minerals and their host diamonds from >660 km depth have C and O isotopic compositions typical of the convecting mantle. This absence of a recycled signature does not support a solely convecting

mantle source, as macrocrystalline diamonds could not have formed unless carbon was liberated from the iron-alloys and iron-carbides that dominate the reduced, volatile-poor lower mantle [2]. We suggest that a decarbonated, but still hydrated slab in the uppermost lower mantle can provide the necessary redox potential to crystallize these diamonds, without disturbing the ambient mantle isotopic signatures. This transition from carbonate slab melting in the transition zone to dehydration in the lower mantle confirms a lower mantle barrier for carbon subduction.

The first seismological images of slabs penetrating the 660 km mantle discontinuity provided evidence for the transport of oceanic slabs into the lower mantle [3]. Nevertheless, the regions of the mantle where volatiles are lost from the slab into the deep convecting mantle remain poorly understood. Diamonds are unique in that they directly sample volatiles from these depths. As high-T fractionation [4] cannot account for all of the isotopic variability observed in sublithospheric diamonds, ^{13}C-depleted signatures of asthenospheric to transition zone diamonds are often interpreted to reflect the deep subduction of sediments, rich in reduced organic carbon [5,6]. This idea has garnered much attention as the deep sequestration of reduced organic carbon in sediments is one hypothesis for the production of Earth's oxidized atmosphere [7]. However, a newly expanded isotopic database implicates carbonates in altered oceanic crust (AOC) as an alternative source for the ^{13}C-depleted signal [8]. The stability of AOC carbonate at depth, until its partial melting between ~ 300 to 700 km [9,10], suggests that it could be a source of carbon in many superdeep diamonds [9,11]. But, thus far, no geochemical signature has clearly related these natural samples to a carbonate-rich AOC protolith. Furthermore, the source of carbon for lower mantle diamonds, a region where carbonate may be exhausted from slabs, is not yet understood.

To evaluate the relative contributions of sediments, AOC, and convecting mantle to the deep mantle carbon cycle, we analyzed a suite of superdeep inclusions in diamond for their δ^{18}O signatures – a system sensitive to the presence of recycled material. Previous measurements of δ^{18}O in superdeep diamonds have been confined to two studies on asthenospheric and transition zone inclusions from the Jagersfontein

kimberlite (South Africa) and the Juina, Collier, and Machado alluvial deposit (Brazil) [12,13]. Here, we report $\delta^{18}O$ from inclusions within a diamond suite from Kankan that carries not only lithospheric and asthenospheric/transition zone garnets, but also low-Al_2O_3 (<1.7 wt. %) orthopyroxene (i.e. former bridgmanite) coexisting with ferropericlase, an assemblage from the uppermost lower mantle (~700 km) [14,15]. Thus, the Kankan diamonds and their silicate inclusions provide powerful means to probe the carbon cycle from lithosphere to lower mantle.

The measured $\delta^{18}O$ and elemental chemistry of lithospheric inclusions from Kankan diamonds are characteristic of their peridotitic and eclogitic substrates. Peridotitic garnet inclusions from Kankan have a $\delta^{18}O$ of +5.3 to +5.7 ‰, within error of the convecting mantle (+5.5 ‰), whereas eclogitic garnets fall between +3.8 to +6.1 ‰, which is within the range of $\delta^{18}O$ reported for mantle eclogite xenoliths (Fig. 1a, c). Thus, diamond forming metasomatic fluids or melts must have had low fluid-melt/rock ratio to not substantially change the $\delta^{18}O$ of the AOC protoliths that exist as eclogite pods within the cratonic mantle.

Unlike lithospheric samples, which can be definitively interpreted as having an eclogitic or peridotitic paragenesis using traditional major elemental classification schemes [16], sublithospheric majoritic garnets are more difficult to separate into parageneses, and are often misclassified [11]. Because of this, we classify the majorites using an experimentally calibrated model, where excess Si^{4+} in the majoritic endmember is charge-balanced with Na^{+} in eclogitic systems, or with divalent cations in Na-poor peridotitic compositions [11]. To quantify this scheme, we derive a parameter, Δperidotite, defined as the difference in divalent cations between the sample and a purely meta-peridotitic majorite, normalized to the difference between the two endmembers. A Δperidotite of 1 represents a purely eclogitic majorite, whereas a Δperidotite of 0 represents a purely meta-peridotitic majorite. The following equation defines the parameter:

$$\Delta\text{peridotite} = \frac{\left|(Mg+Ca+Fe+Mn)_s-(m_p(Si+Ti)_s+b_p)\right|}{\left|(m_b(Si+Ti)_s+b_e-(m_p(Si+Ti)_s+b_p)\right|} \quad \text{Equation 1}$$

where *m* is the slope of the endmember substitution, *b* is the y-intercept of the endmember, *p* and *e* are the meta-peridotite and eclogitic endmembers, respectively, and *s* is the majoritic sample.

The majority of majoritic garnet inclusions lie between these end-member trends ($0 < \Delta\text{peridotite} < 1$), an intermediate composition termed "meta-pyroxenitic" (Fig. 2a) [11]. Because these meta-pyroxenitic inclusions are intermediate in major element composition, we might also expect their $\delta^{18}O$ to be intermediate compared to the values reported for lithospheric eclogitic and peridotitic garnets. Instead, meta-pyroxenitic majoritic garnets from Kankan have much more extreme $\delta^{18}O$ (+9.1 to +10.5 ‰) than the Kankan eclogitic garnet inclusions of lithospheric origin (+3.8 to +6.1 ‰). Meta-pyroxenitic majorites from the Juina region (Brazil) [13] and Jagersfontein (S. Africa) diamonds [12] also have a significantly higher $\delta^{18}O$ mode than eclogitic garnet inclusions in diamonds worldwide (Fig. 1c), and extend to even more extreme values (+12 ‰) . Because no majorite inclusion in diamond has yet been measured with $\delta^{18}O$ of < +7.5 ‰ (n=24) and only 4% of data from a composite model of AOC approaches the median $\delta^{18}O$ of majorites [17], with < 0.05% extending to +12 ‰, we infer that there must be a unique source for the highly elevated $\delta^{18}O$ in meta-pyroxenitic superdeep inclusions.

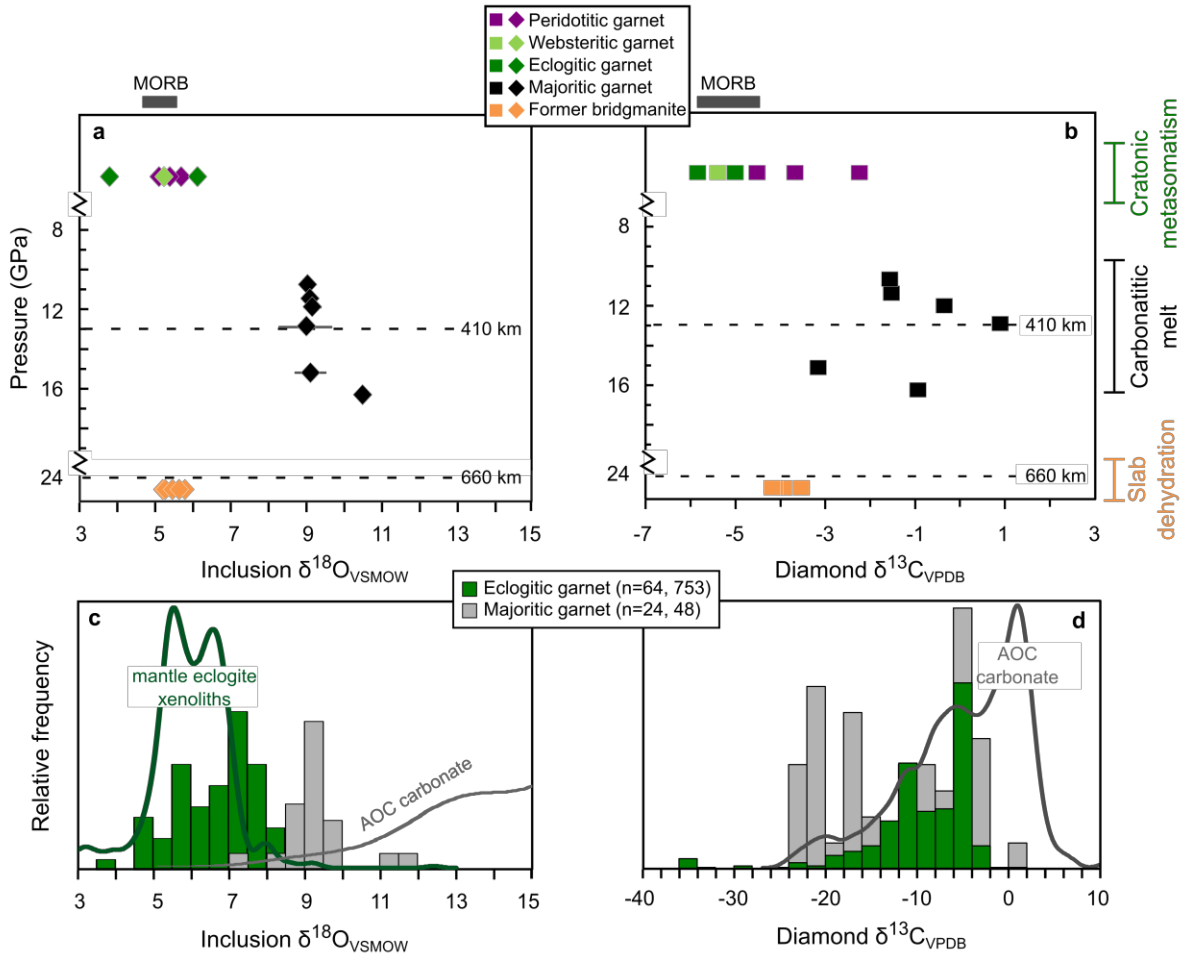

Figure 1. (a) Oxygen isotope composition ($\delta^{18}O_{VSMOW} = ((\frac{^{18}O}{^{16}O})_{sample}/(\frac{^{18}O}{^{16}O})_{VSMOW} - 1)\ x\ 1000\ ‰$) of silicate inclusions and **(b)** carbon isotope composition ($\delta^{13}C_{PDB} = ((\frac{^{13}C}{^{12}C})_{sample}/(\frac{^{13}C}{^{12}C})_{PDB} - 1)\ x\ 1000‰$) for diamond hosts [18] versus depth for a suite of Kankan diamonds. Errors are 2σ standard deviation. Pressure and depth estimates are plotted for majoritic garnets [19], whereas formation depth for retrogressed bridgmanites is determined based on their low Al content [15]. MORB oxygen and carbon isotopic ranges are indicated above graphs [20–23]. Interpreted environments of formation are indicated on the right. **(c)** $\delta^{18}O$ histograms for eclogitic [17,24,25] and majoritic garnet [12,13] inclusions. Also plotted are probability density functions (PDF, bandwidth of 0.2 ‰) of eclogitic garnets from mantle xenoliths [26] and AOC carbonates (bandwidth of 1.9 ‰) [8]. Note that eclogitic and majoritic garnet inclusions have different modes, with majoritic garnets shifted towards higher $\delta^{18}O$ values. **(d)** $\delta^{13}C$ histograms of eclogitic and majoritic garnet-bearing diamonds, and a PDF (bandwidth of 1.17 ‰) for AOC carbonate [8]. See supplementary references. The scale is different to that in Fig. 1b.

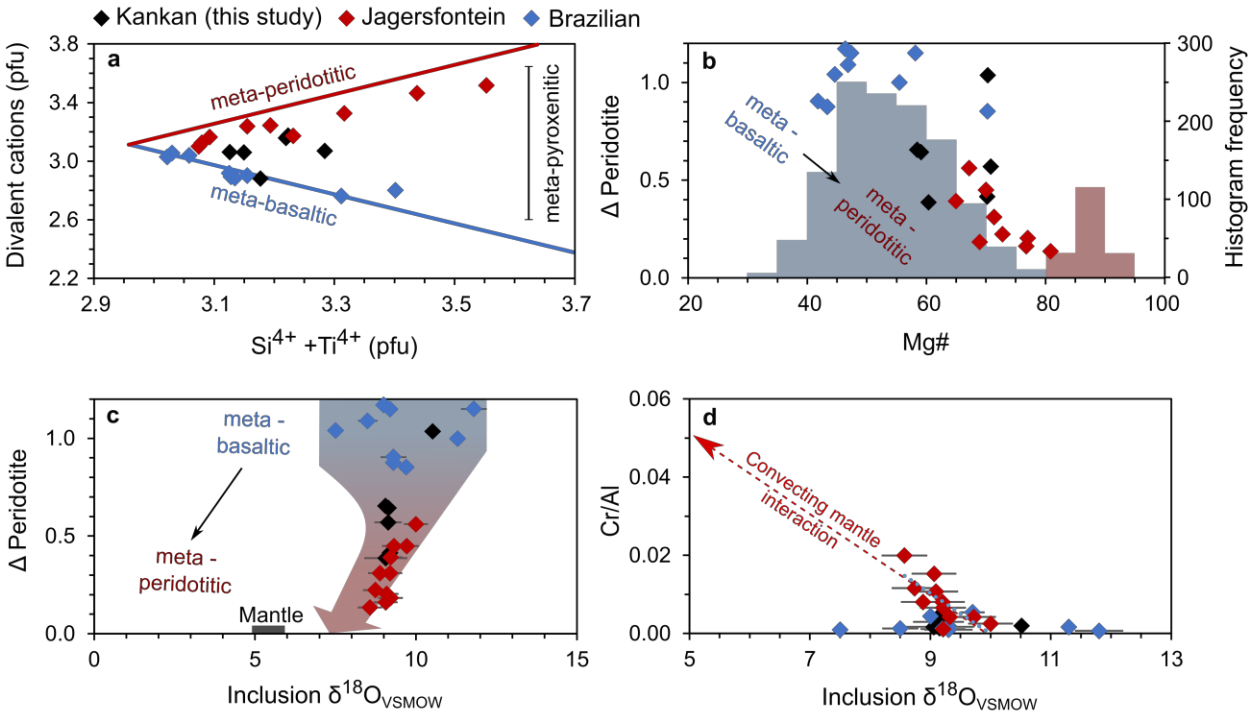

Figure 2. (a) Divalent cations (Fe_{total}, Mg, Ca, Mn) versus Si and Ti per formula unit ([O]=12) in Kankan, Jagersfontein, and Juina region majorites (after Kiseeva et al., 2013). Red line is the substitution typical for meta-peridotitic associations. Blue line is the substitution typical for meta-basaltic/eclogitic compositions. Substitution lines begin at the median value for eclogitic garnets (Si + Ti of 2.96, divalent cations of 3.11) [27]. **(b)** Majorite Mg# and the parameter Δperidotite, which indicates an individual inclusion's deviation from the meta-peridotitic substitution (Δperidotite of 0 is meta-peridotitic, Δperidotite of 1 is meta-basaltic/eclogitic). The histogram and the secondary axis show the distribution in Mg# of lithospheric eclogitic and peridotitic garnet inclusions (blue and red histograms respectively; see supplementary references). **(c)** $\delta^{18}O$ versus Δperidotite values of majorites. Arrows trends from purely eclogitic compositions (high Δperidotite) towards more meta-peridotitic compositions (low Δperidotite). **(d)** Cr/Al and $\delta^{18}O$ in majorites trends from eclogitic majorites (low Cr/Al) to more meta-peridotitic majorites with lower $\delta^{18}O$. Red line is a linear regression ($r^2 = 0.6$) for the Jagersfontein data. Errors are 2σ standard deviation.

Two potential reservoirs of high $\delta^{18}O$ include sediments and AOC. Both reservoirs contain distinct carbon-bearing constituents. Sediments are generally dominated by "marine carbonate", but may be locally enriched in organic carbon from marine and terrestrial organisms living near continental margins, called "reduced organic-rich carbon" [1]. In comparison, much of the carbon present in AOC carbon is the carbonate which precipitated in equilibrium with dissolved inorganic carbon (DIC), called "DIC-equilibrium carbonate" [8]. However, recent studies have documented that AOC also includes carbonate precipitated from biologically/kinetically fractionated DIC [8]. We call this ^{13}C-depleted endmember "biogenic AOC carbonate".

The recent identification of ^{13}C-depleted biogenic AOC carbonate [8] challenges the assumption that ^{13}C depleted diamonds must originate from deeply subducted sediment [4,6]. In order to further examine the source of the ^{13}C-depleted and ^{18}O-enriched signal, we examine the database of $\delta^{15}N$ in diamond (Fig. 3) - a less ambiguous isotopic tracer to discriminate between AOC and sediment sources. We find that nearly 20% of all eclogitic diamonds have lower $\delta^{15}N$ than the mantle (-5 ± 2 ‰), and >80% have $\delta^{15}N < 0$, suggesting that the subducted endmember must have strongly negative $\delta^{15}N$. Organic-rich sediments cannot satisfy this requirement, as their $\delta^{15}N$ values are almost exclusively positive [28], but AOC spans a large range of $\delta^{15}N$ (-12 to +10 ‰), reflecting ^{15}N depletion in high-T clays and ^{15}N enrichment in low-T clays [29,30]. Thus, following Li et al. (2019), we suggest that the large isotopic field that defines most eclogitic diamonds is defined by mixing between three AOC endmembers: 1) nitrogen-bearing high-T clay with mantle-derived carbon, 2) nitrogen-bearing low-T clay with biogenic AOC carbonate or 3) nitrogen-bearing low-T clay with DIC-equilibrium carbonate [8]. This importance of AOC for diamond formation is demonstrated only for lithospheric diamonds, but if sediment is uncommon as a carbon source at these shallow depths, it is likely to be even scarcer in the asthenosphere and transition zone. Interestingly, we note that all published asthenospheric and transition zone diamonds have $\delta^{15}N > 0$ (Fig. 3), suggesting that diamond formation in that region of the mantle is driven strictly by the uppermost, low-T AOC (i.e. endmembers 2 and 3).

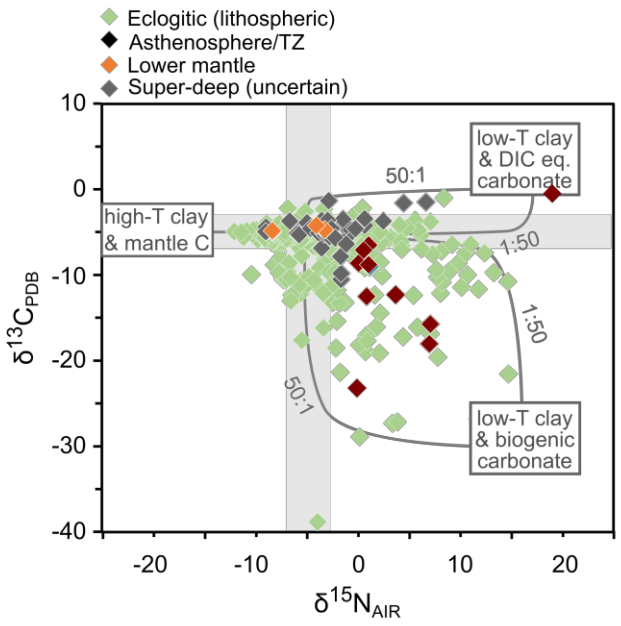

Figure 3. Worldwide database of $\delta^{13}C$ and $\delta^{15}N$ for eclogitic diamonds of lithospheric origin and those of superdeep origin. The convecting upper mantle isotopic signature is represented by the grey bands. Also indicated are the three endmembers produced from five different constituents – ^{15}N depleted high-T clay, ^{15}N enriched low-T clay, convecting mantle carbon, and carbon from DIC-equilibrium carbonate and biogenic AOC carbonate [8]. Mixing lines between the endmembers and the mantle are N/C_{mantle} / N/C_{AOC} of 50:1 and 1:50 (see discussion in ref [8]). Superdeep diamonds include those of asthenospheric and transition zone (TZ) origin (majorite and Ca-silicate inclusions), lower mantle origin (ferropericlase + $MgSiO_3$/$CaSiO_3$ inclusions), and diamonds of uncertain super-deep origin (e.g., ferropericlase inclusions). Note that asthenospheric/TZ diamonds have exclusively positive $\delta^{15}N$, but variable $\delta^{13}C$. Errors are smaller than symbols.

A carbonate-rich AOC origin for diamond is further supported by our study of majoritic inclusions. Not only are the majoritic inclusions offset towards the higher $\delta^{18}O$ values recorded in carbonates (Fig. 1c), but the formation depths of these majorites (7-19 GPa; Fig S4) also correlate well with the experimentally-derived pressures at which carbonated slabs melt (9-21 GPa [31]). These experiments demonstrate that the carbonatitic melt derived from the slab will crystallize both majoritic garnet and diamond after injection into and reaction with the surrounding reduced convecting mantle [9,10,32]. The high-

Na, low Cr and Mg# majorites reflect crystallization products from slab carbonatite that experienced little mantle contamination (i.e. high melt/rock ratios) and short migration paths before redox freezing (Fig. 2b, d). Increasing reaction between the melt and the convecting mantle (melt/mantle <2; Fig. S3) gradually raises the Cr content and the Mg# of the majorites towards peridotitic values. Thus, this reaction between AOC derived carbonatite and convecting mantle accounts for the intermediate "mixed" elemental compositions of these majoritic garnets.

The importance of AOC as a source for lithospheric to transition zone diamonds has implications for the efficiency with which carbon is recycled within Earth's mantle. The absence of a clear sedimentary carbon signal at diamond-forming depths suggests that sedimentary volatiles may be recycled back to the surface during arc volcanism or stored in shallow accretionary prisms [5]. This observation is at odds with the hypothesis that an oxidized atmosphere could have been produced at ~2.5 Ga due to the deep subduction and sequestration of reduced sedimentary carbon [1,7]. Instead, an oxidized atmosphere must have been produced via other means (see [33] for review of possible mechanisms).

Whereas the strong ^{18}O enrichment in majoritic garnets can be related to a carbonated slab in the asthenosphere/transition zone, the first $\delta^{18}O$ measurements of a lower mantle retrogressed bridgmanites show negligible oxygen from recycled crust. Instead, their $\delta^{18}O$ (+5.3 to +5.8 ‰), host diamond $\delta^{13}C$ (-3.5 to -4.1 ‰ [18]), and average Mg# (95.0 and 86.7 for bridgmanite and associated ferropericlase inclusions, respectively) are all indicative of a fertile pyrolite-like composition (Table S3) [34,35]. This lack of a crustal signature is unusual in sublithospheric diamonds [36], likely because diamond is rarely stable in the metal-bearing convecting mantle that is found at > 8 GPa [37], unless C concentrations are extremely elevated above typical (~50 ppm) [2,38]. Since the convecting lower mantle has ~1 wt. % metal [37], and likely no more than 50 ppm C, iron metal is the dominant carbon-bearing phase [2,38]. In order to produce macrocrystalline lower mantle diamonds [39], their constituent carbon needs to be liberated and locally concentrated. Metal alloys at lower mantle pressures have been shown to be unstable in a hydrated

191 environment [40], indicating that other carbon-bearing phases, such as diamond, will become more stable.
192 The final stages of slab dehydration occur in the uppermost lower mantle [41] and would introduce
193 negligible non-convecting mantle oxygen (i.e. slab-derived H_2O) into the system. Therefore, we propose
194 that carbonate-depleted, but still hydrated, subducting oceanic slabs can supply the necessary redox
195 gradients and metasomatic mobilization of ambient carbon for lower mantle diamond formation, without
196 extensively changing the original ambient mantle isotopic signature.
197
198 The contrasting isotopic composition of diamonds and their silicate inclusions at lithospheric, transition
199 zone, and lower mantle depths suggest profound differences in modes of diamond formation, and the
200 behavior of volatiles through these mantle regions. Here we document geochemical evidence for the deep
201 cycling of carbonate in AOC and its role in forming both lithospheric and superdeep diamonds, and their
202 inclusions. In contrast, diamonds from the uppermost lower mantle show no trace of a subducted
203 signature, and may have crystallized after a dehydrating slab triggered carbon liberation from metallic
204 hosts in the surrounding mantle. The transition from diamond formation in a slab-derived carbonatitic
205 medium in the transition zone to carbonate-free slab dewatering in the ambient lower mantle is consistent
206 with the notion that it is difficult to transport crustal carbonates to lower mantle depths along reasonable
207 slab thermal trajectories [9], and suggests that there may indeed be a barrier to carbon subduction above the
208 lower mantle.

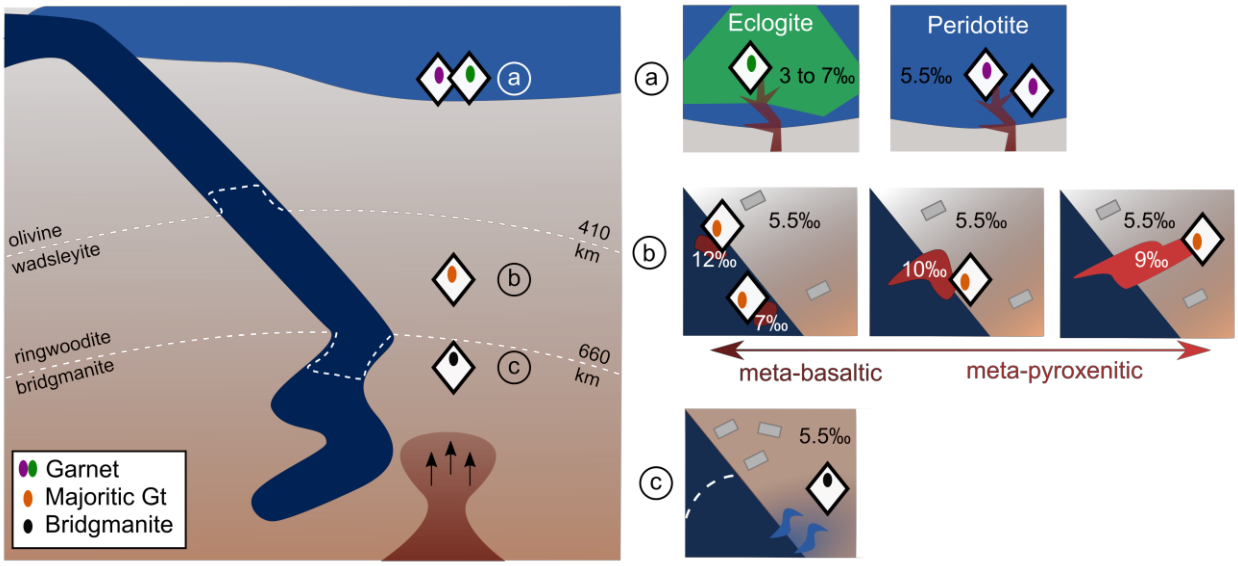

Figure 4. Diamonds formed in the lithosphere, transition zone, and lower mantle are brought to the surface by convective mantle circulation, plume ascent, and/or kimberlitic magmatism. **(a)** Lithospheric diamond forms by fluid or melt metasomatism of eclogitic and peridotitic substrates. The range in $\delta^{18}O$ for eclogitic and peridotitic garnet inclusions is buffered by the host rocks, because of low fluid-melt/rock ratios. **(b)** In the transition zone, a carbonated subducting oceanic slab is heated above its solidus temperature to produce carbonatite. Diamonds and majoritic garnets inclusions crystallize during the reaction between the carbonatitic melt and the reduced convecting mantle. High melt/rock ratios and short migration paths produce majorite inclusions with meta-basaltic compositions and extreme $\delta^{18}O$ values, directly reflecting the local melt sources (carbonated AOC). Longer melt migration paths into the mantle "hanging wall" lead to interaction with larger volumes of convecting mantle, which is reflected in the lower $\delta^{18}O$ and increasingly ultrabasic, meta-pyroxenitic character of the majorite inclusions. **(c)** As the slab penetrates into the lower mantle, the negative pressure-temperature slope (i.e. Clapeyron slope) of the post-spinel transition [42,43] and the delayed garnet to perovskite transition in metabasaltic lithologies [44] retards the formation of lower mantle minerals (dotted white line). The transition to a lower mantle mineralogy leads to slab dehydration and hydration of the surrounding mantle. The hydrated ambient mantle releases carbon from its metallic iron hosts to form diamond.

References

1. Plank, T. & Manning, C. E. Subducting carbon. *Nature* **574**, 343–352 (2019).
2. Dasgupta, R. & Hirschmann, M. M. The deep carbon cycle and melting in Earth's interior. *Earth Planet. Sci. Lett.* **298**, 1–13 (2010).
3. Creager, K. C. & Jordan, T. H. Slab penetration into the lower mantle. *J. Geophys. Res.* **89**, 3031–3049 (1984).
4. Cartigny, P. Stable Isotopes and the Origin of Diamond. *Elem.* **1**, 79–84 (2005).
5. Kelemen, P. B. & Manning, C. E. Reevaluating carbon fluxes in subduction zones, what goes down, mostly comes up. *PNAS* **112**, (2015).
6. Sobolev, V. S. & Sobolev, N. V. New proof on very deep subsidence of eclogitized crustal rocks. *Dokl. Acad. Sci. USSR, Earth Sci. Sect.* **250**, 88–90 (1982).
7. Duncan, M. S. & Dasgupta, R. Rise of Earth's atmospheric oxygen controlled by efficient subduction of organic carbon. *Nat. Geosci.* **10**, 387–392 (2017).
8. Li, K., Li, L., Pearson, D. G. & Stachel, T. Diamond isotope compositions indicate altered igneous oceanic crust dominates deep carbon recycling. *Earth Planet. Sci. Lett.* **516**, 190–201 (2019).
9. Thomson, A. R., Walter, M. J., Kohn, S. C. & Brooker, R. A. Slab melting as a barrier to deep carbon subduction. *Nature* **529**, 76–79 (2016).
10. Walter, M. J. *et al.* Primary carbonatite melt from deeply subducted oceanic crust. *Nature* **454**, 622–625 (2008).
11. Kiseeva, E. S. *et al.* Metapyroxenite in the mantle transition zone revealed from majorite inclusions in diamonds. *Geology* **41**, 883–886 (2013).
12. Ickert, R. B., Stachel, T., Stern, R. A. & Harris, J. W. Extreme 18O-enrichment in majorite constrains a crustal origin of transition zone diamonds. *Geochemical Perspect.*

Lett. **1**, 65–74 (2015).

13. Burnham, A. D. *et al.* Stable isotope evidence for crustal recycling as recorded by superdeep diamonds. *Earth Planet. Sci. Lett.* **432**, 374–380 (2015).

14. Stachel, T., Brey, G. P. & Harris, J. W. Kankan diamonds (Guinea) I: from the lithosphere down to the transition zone. *Contrib. to Mineral. Petrol.* **140**, 1–15 (2000).

15. Stachel, T., Harris, J. W., Brey, G. P. & Joswig, W. Kankan diamonds (Guinea) II: lower mantle inclusion parageneses. *Contrib. to Mineral. Petrol.* **140**, 16–27 (2000).

16. Grütter, H. S., Gurney, J. J., Menzies, A. H. & Winter, F. An updated classification scheme for mantle-derived garnet, for use by diamond explorers. *Lithos* **77**, 841–857 (2004).

17. Ickert, R. B., Stachel, T., Stern, R. A. & Harris, J. W. Diamond from recycled crustal carbon documented by coupled δ18O-δ13C measurements of diamonds and their inclusions. *Earth Planet. Sci. Lett.* **364**, 85–97 (2013).

18. Stachel, T., Harris, J. W., Aulbach, S. & Deines, P. Kankan diamonds (Guinea) III: δ13C and nitrogen characteristics of deep diamonds. *Contrib. to Mineral. Petrol.* **142**, 465–475 (2002).

19. Beyer, C. & Frost, D. J. The depth of sub-lithospheric diamond formation and the redistribution of carbon in the deep mantle. *Earth Planet. Sci. Lett.* **461**, 30–39 (2017).

20. Cooper, K. M., Eiler, J. M., Sims, K. W. W. & Langmuir, C. H. Distribution of recycled crust within the upper mantle: Insights from the oxygen isotope composition of MORB from the Australian-Antarctic Discordance. *Geochem. Geophys. Geosyst.* **10**, Q12004 (2009).

21. Cooper, K. M., Eiler, J. M., Asimow, P. D. & Langmuir, C. H. Oxygen isotope evidence

for the origin of enriched mantle beneath the mid-Atlantic ridge. *Earth Planet. Sci. Lett.* **220**, 297–316 (2004).

22. Eiler, J. M., Schiano, P., Kitchen, N. & Stolper, E. M. Oxygen-isotope evidence for recycled crust in the sources of mid-ocean-ridge basalts. *Nature* **403**, 530–534 (2000).

23. Marty, B. & Zimmermann, L. Volatiles (He, C, N, Ar) in mid-ocean ridge basalts: Assesment of shallow-level fractionation and characterization of source composition. *Geochim. Cosmochim. Acta* **63**, 3619–3633 (1999).

24. Schulze, D. J. *et al.* Anticorrelation between low δ13C of eclogitic diamonds and high δ18O of their coesite and garnet inclusions requires a subduction origin. *Geology* **41**, 455–458 (2013).

25. Zedgenizov, D., Rubatto, D., Shatsky, V., Ragozin, A. & Kalinina, V. Eclogitic diamonds from variable crustal protoliths in the northeastern Siberian craton: Trace elements and coupled δ13C–δ18O signatures in diamonds and garnet inclusions. *Chem. Geol.* **422**, 46–59 (2016).

26. Korolev, N. M., Melnik, A. E., Li, X. H. & Skublov, S. G. The oxygen isotope composition of mantle eclogites as a proxy of their origin and evolution: A review. *Earth-Science Rev.* **185**, 288–300 (2018).

27. Beard, B. L. *et al.* Petrography and geochemistry of eclogites from the Mir kimberlite, Yakutia, Russia. *Contrib. Miner. Pet.* **125**, 293–310 (1996).

28. Li, L., Zheng, Y. F., Cartigny, P. & Li, J. Anomalous nitrogen isotopes in ultrahigh-pressure metamorphic rocks from the Sulu orogenic belt: Effect of abiotic nitrogen reduction during fluid-rock interaction. *Earth Planet. Sci. Lett.* **403**, 67–78 (2014).

29. Li, L., Bebout, G. E. & Idleman, B. D. Nitrogen concentration and δ15N of altered

oceanic crust obtained on ODP Legs 129 and 185: Insights into alteration-related nitrogen enrichment and the nitrogen subduction budget. *Geochim. Cosmochim. Acta* **71**, 2344–2360 (2007).

30. Busigny, V., Laverne, C. & Bonifacie, M. Nitrogen content and isotopic composition of oceanic crust at a superfast spreading ridge: A profile in altered basalts from ODP Site 1256, Leg 206. *Geochemistry, Geophys. Geosystems* **6**, (2005).

31. Kiseeva, E. S., Litasov, K. D., Yaxley, G. M., Ohtani, E. & Kamenetsky, V. S. Melting and Phase Relations of Carbonated Eclogite at 9–21 GPa and the Petrogenesis of Alkali-Rich Melts in the Deep Mantle. *J. Petrol.* **54**, 1555–1583 (2013).

32. Bobrov, A. V, Litvin, Y. A., Bindi, L. & Dymshits, A. M. Phase relations and formation of sodium-rich majoritic garnet in the system Mg3Al2Si3O12–Na2MgSi5O12 at 7.0 and 8.5 GPa. *Contrib. Miner. Pet.* **156**, 243–257 (2008).

33. Sessions, A. L., Doughty, D. M., Welander, P. V., Summons, R. E. & Newman, D. K. The Continuing Puzzle of the Great Oxidation Event. *Current Biology* **19**, R567–R574 (2009).

34. Cartigny, P., Palot, M., Thomassot, E. & Harris, J. W. Diamond Formation: A Stable Isotope Perspective. *Annu. Rev. Earth Planet. Sci.* **42**, 699–732 (2014).

35. Wood, B. J. Phase transformations and partitioning relations in peridotite under lower mantle conditions. *Earth Planet. Sci. Lett.* **174**, 341–354 (2000).

36. Stachel, T. Diamonds from the asthenosphere and the transiton zone. *Eur. J. Miner.* **13**, 883–892 (2001).

37. Frost, D. J. & Mccammon, C. A. The Redox State of Earth's Mantle. (2008). doi:10.1146/annurev.earth.36.031207.124322

38. Rohrbach, A., Ghosh, S., Schmidt, M. W., Wijbrans, C. H. & Klemme, S. The stability of

Fe-Ni carbides in the Earth's mantle: Evidence for a low Fe-Ni-C melt fraction in the deep mantle. *Earth Planet. Sci. Lett.* **388**, 211–221 (2014).

39. Smith, E. M. *et al.* Large gem diamonds from metallic liquid in Earth's deep mantle. *Science (80-.).* **354**, 1403–1405 (2016).

40. Zhu, F., Li, J., Liu, J., Dong, J. & Liu, Z. Metallic iron limits silicate hydration in Earth's transition zone. *Proc. Natl. Acad. Sci. U. S. A.* **116**, 22526–22530 (2019).

41. Schmandt, B., Jacobsen, S. D., Becker, T. W., Liu, Z. & Dueker, K. G. Dehydration melting at the top of the lower mantle. *Science (80-.).* **344**, 1265–1268 (2014).

42. Ono, S., Hirose, K., Kikegawa, T. & Saito, Y. The compressibility of a natural composition calcium ferrite-type aluminous phase to 70 GPa. *Phys. Earth Planet. Inter.* **131**, 311–318 (2002).

43. Hirose, K. Phase transitions in pyrolitic mantle around 670-km depth: Implications for upwelling of plumes from the lower mantle. *J. Geophys. Res. Solid Earth* **107**, ECV 3-1-ECV 3-13 (2002).

44. Irifune, T. & Ringwood, A. E. Phase transformations in a harzburgite composition to 26 GPa: implications for dynamical behaviour of the subducting slab. *Earth Planet. Sci. Lett.* **86**, 365–376 (1987).

45. Ickert, R. B. & Stern, R. A. Matrix Corrections and Error Analysis in High-Precision SIMS18O/16O Measurements of Ca–Mg–Fe Garnet. *Geostand. Geoanal. Res.* **37**, 429–448 (2013).

46. Wang, Z., Bucholz, C., Skinner, B., Shimizu, N. & Eiler, J. Oxygen isotope constraints on the origin of high-Cr garnets from kimberlites. *Earth Planet. Sci. Lett.* **312**, 337–347 (2011).

47. Mattey, D., Lowry, D. & Macpherson, C. Oxygen isotope composition of mantle peridotite. *Earth Planet. Sci. Lett.* **128**, 231–241 (1994).

Acknowledgements The authors acknowledge NSERC and the Deep Carbon observatory for funding this study. The Diamond Trading Company (a member of the DeBeers Group of Companies) is thanked for the donation to JWH of the diamonds used in this study.

Author Contributions M.E.R. and R.S. collected the data. M.E.R. provided the initial data interpretation and manuscript and input from all other authors improved the interpretation and writing.

Competing Interests The authors declare no competing interests.

Data Availability All data generated or analysed during this study are included in this published article (and its supplementary information files). Accession codes for databases of previously published data utilized here will be made available upon publication.

Materials & Correspondence. Direct requests for materials and correspondence to M.E.R. (margoregier@gmail.com)

Methods

Enstatite and garnet inclusions in diamond were analyzed using a Cameca IMS 1280 multicollector ion microprobe with ~2 nA $^{33}Cs^-$ primary beam and 20 keV impact energy. Analytical methods and standards for garnets are detailed by Ickert and Stern (2013). The presence of high-Cr_2O_3 lithospheric garnets required the development of a new matrix correction. Olivine and high-Cr_2O_3 garnet pairs from depleted peridotite xenoliths were cast into epoxy and pressed into indium mounts along with garnet and olivine reference material. Olivine $\delta^{18}O$ values were all within error of mantle values, suggesting that associated garnets should be also within the expected normal mantle $\delta^{18}O$ range. Instead, a plot of garnet Cr_2O_3 vs. $\delta^{18}O$ defines a positive slope that reaches ~1 ‰ above the mantle range at high Cr_2O_3 contents (Fig. S1). A Cr-related matrix effect has been previously suggested [46], but variable laser fluorination yields of Cr-rich minerals have inhibited a robust determination of the calibration. Our method bypasses the need for laser fluorination of high Cr-garnets, being instead based on laser fluorination of a low Cr-garnet (S0068) and a reasonable assumption of mineral isotopic equilibrium at mantle temperatures. The 95% confidence uncertainty estimates for $\delta^{18}O_{VSMOW}$ for garnets average ±0.29 ‰. Enstatite $\delta^{18}O$ measurements also required the development of a new calibration for Mg# using laser fluorination results [47] for sample F866 (94.1 Mg#) and CCIM standard S0170 (91.2 Mg#). For analyses of unknown enstatites, the 95% confidence uncertainty estimates for $\delta^{18}O_{VSMOW}$ average ±0.21 ‰. Adjacent to each ion probe crater, major element data were collected on a Cameca SX100 with 5 wavelength dispersive spectrometers at 20 keV energy, 20 nA of beam current at 1 μm diameter. The counting time was 30 seconds for all elements. Detection limits are available in Table S1 and standards are reported in Table S2.